LOCAL HEAT TRANSFER COEFFICIENTS IN SCRAPED-FILM HEAT EXCHANGER

HISASHI MIYASHITA
Department of Chemical Engineering, Toyama University, Takaoka 933
TERRENCE W. HOFFMAN
Department of Chemical Engineering, McMaster University, Hamilton, Ontario, Canada L8S 4L7

The instantaneous heat transfer coefficients in a scraped-film heat exchanger have been determined using the electrochemical technique for a two-bladed, 78.7 mm I.D. exchanger. The time-averaged local heat transfer coefficients were found to agree fairly well with previous work of Azoory and Bott, though some variation in liquid flow rate was detected. The time-averaged local Nusselt number was found to be represented by

$$Nu=0.15(Re_r\cdot Pr)^{1/2}Re_w^a$$

with $a=(1-3.74\times10^{-2}N)/9$. The variation of heat transfer coefficient with time was observed to be very different from that predicted by the accepted model for the phenomena based upon unsteady state conduction.

In a scraped-film heat exchanger, the liquid film is subjected to gravitational and centrifugal forces as the blades rotate and scrape it from the outer heat transfer surface. At the same time, fresh material is exposed to a clean heat transfer surface. The fluid mechanical and heat transfer phenomena occurring in such a system are very complex and hence any analysis of the heat transfer mechanisms must be based on a simplified model for these phenomena.

The object of this study was to measure indirectly the instantaneous heat transfer rate at points in the exchanger in order to elucidate the actual behavior in such systems. This was done using the electrochemical method developed for such studies[10]. The main advantage of such a system is that it provides an instantaneous mass transfer rate uncomplicated by thermal or mass capacity effects. The analogy between heat and mass transfer allows translation of the mass transfer rate to a heat transfer rate (or coefficient).

Many investigators have studied the scraped-film heat exchanger. For instance, Kern and Karakas[7] and Lustenader *et al.*[9] have postulated that heat is transferred through the film by steady-state molecular conduction. Kool[8] and Harriot[5] suggest that the rate of heat transfer depends more on the rate of transient conduction in a frequently renewed layer than on the rate of steady-state conduction through the entire film. This model is very similar to the penetration surface-renewal models (penetration theory model) of Higbie[6]. In this model, as originally proposed by Kool[8], the heat transfer coefficient is calculated from the relationship

$$h(T_w-T_b)=-k(dT/dx)_{x=0} \tag{1}$$

where the derivative is obtained from the solution of the transient conduction equation:

$$(\partial T/\partial\theta)=\alpha(\partial^2T/\partial x^2) \tag{2}$$

as applied to the process liquid. The time-averaged local heat transfer coefficient is obtained by integrating Eq. (1) over the contact time θ_c to yield

$$h=\frac{2}{\sqrt{\pi}}\left(\frac{C_p\rho k}{\theta_c}\right)^{1/2} \tag{3}$$

where $\theta_c=1/nN$, which upon simplifying becomes

$$h=1.128(\rho C_p knN)^{1/2} \tag{4}$$

which, in dimensionless terms, becomes

$$Nu=1.128(Re_r\cdot Pr)^{1/2} \tag{5}$$

This model predicts that the heat transfer coefficient is a function of the physical properties of the fluid, the rotational speed and the number of blades; it does not predict a size dependence nor a dependence of mass flow rate.

In an extensive study, Azoory and Bott[1] have tried to relate the time-averaged local heat transfer coefficient, as measured by a plug-type flux meter, to the penetration model. From their experimental measurements, they developed an empirical correction

Received February 16, 1978. Correspondence concerning this article should be addressed to H. Miyashita.

factor, which was found to be a function of Prandtl number, to make their results agree with the model formulation, viz:

$$h=1.128(\rho C_p knN)^{1/2}\cdot(1/f) \qquad (6)$$

where $f=(Pr/500)+3.50$

Average film heat transfer coefficients have been reported[9] for heat transfer experiments in which heat is transferred over the entire transfer surface. Bott *et al.*[2] point out, however, that axial dispersion effects may occur and hence the calculation of heat transfer coefficients based on familiar log-mean temperature difference (plug-flow model) may be suspect under some conditions. They present a method of estimating the error in such apparent coefficients. They also present an empirical equation for calculating the time-averaged coefficient which shows some dependence on the mass flow rate of liquid. It should be pointed out that in the design of such exchangers the area is normally calculated based on the plug-flow model.

1. Experimental Apparatus and Procedure

This experimental program is based on the electrochemical method for measuring instantaneous mass transfer rates at a transfer surface. It employs the redox reaction of ferrocyanide/ferricyanide ions in an electrolytic solution (aqueous caustic solution) at nickel electrodes.

The schematic diagram of the experimental apparatus is shown in **Fig. 1**. The electrolyte was pumped from a storage reservoir [1] to a constant head tank [3] by a Teflon gear pump [2]. The electrolyte then flowed through a flow central needle valve [4], a rotameter and a heater [6] (for temperature control) and then through the scraped-film exchanger [8] back to the reservoir. To avoid oxidation of the ferrocyanide solution, nitrogen gas blanketed the storage tanks. The rotation speed of the wiper was controlled by a variable-speed motor control [7]. All flow lines were made of type 316 stainless steel or plastic tubing to minimize corrosion effects.

Figure 2 indicates the details of the scraped-film exchanger and the circuitry for measuring the current (and hence the mass transfer coefficient). The exchanger consists of a 78.7 mm I.D. by 457.2 mm long nickel-plated copper tube; the wall thickness was 6.4 mm. A central shaft (13 mm diameter) housed two fixed wiper blades made from nylon. Four isolated nickel electrodes (cathodes), the details of which are shown in Fig. 2, were located at 88.9 mm, 165.1 mm, 241.3 mm and 342.9 mm from the top on the same vertical axis. The rest of the tube was used as the anode. Great care was exercised in constructing the tube. It was honed to ensure that it was

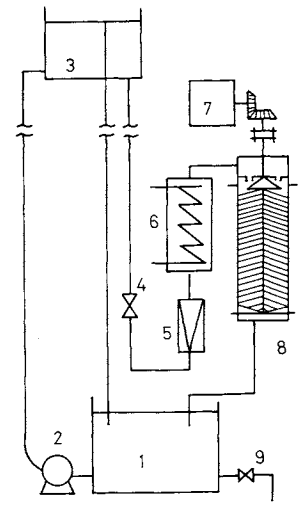

1. storage tank 2. pump 3. constant-head tank
4. valve for adjusting flow rate 5. rotameter 6. heater
7. motor with variable speed 8. heat exchanger
9. drain valve

Fig. 1 Layout of experimental apparatus

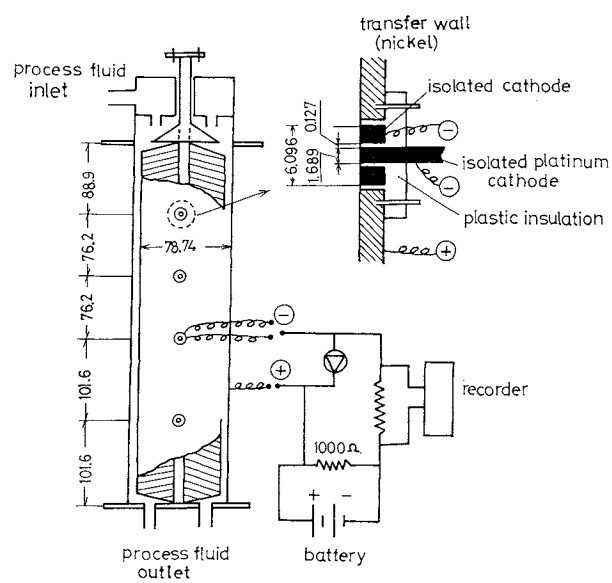

Fig. 2 Details of scraped-film exchanger, electrode and electrical circuitry

circular and that the shaft containing the blades was located accurately on the centerline. The clearance between blades and tube was accurately set at 0.127 mm (0.005 in.).

The instantaneous current through a given electrode was measured by measuring the instantaneous voltage across a known resistance. This voltage was recorded by a Minneapolis-Honeywell Viscorder (recording oscillograph) which employs mirror galvanometers with high frequency response.

All measurements were made with the fluid temperature at 30°C (±0.5°C). The compositions and physical properties of the electrolyte solution and the range

Table 1 Experimental Information

Composition of electrolyte solution	
$K_4Fe(CN)_6$	0.005 mol/*l*
$K_3Fe(CN)_6$	0.005 mol/*l*
NaOH	2 N
Physical properties of electrolyte solution (at 30°C)	
density ρ	1081.6 kg/m^3
specific heat C_p	3786.5 J/kg·K
thermal conductivity k	0.644 W/m·K
diffusivity D	5.62×10^{-10} m^2/s
viscosity μ	0.00124 N·s/m^2
Range of experimental conditions	
solution temperature	30°C ($\pm$0.5°C)
mass flow rate	$24\text{–}80\times10^{-3}$ kg/s
rotational speed	0.78–18 s^{-1}
Re_w	261–1032
Re_r	$8.64\times10^3\text{–}1.86\times10^5$

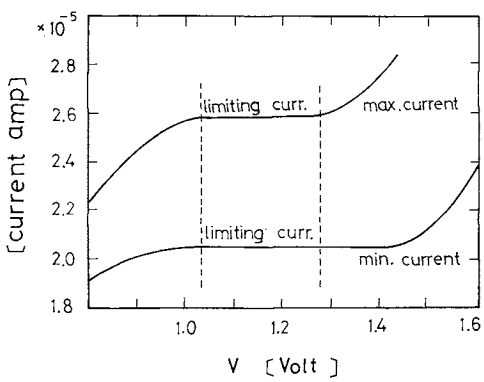

Fig. 3 Experimental results to determine limiting current region: plot of cathode current versus applied voltage across electrodes

of experimental conditions are given in **Table 1**.

2. Calculation of Transfer Coefficients

The mass transfer coefficients were measured by using the ferricyanide/ferrocyanide redox electrochemical reaction in which

$$Fe(CN)_6^{-3}+e^-\rightarrow Fe(CN)_6^{-4} \quad \text{[at cathode]}$$

$$Fe(CN)_6^{-4}\rightarrow Fe(CN)_6^{-3}+e^- \quad \text{[at anode]}$$

The method has been reviewed in detail by Mizushina[10].

The basis of the method is that when operating at the so-called "limiting current" condition the electrochemical phenomena are limited by mass transfer at the cathode only, and hence the concentration of ferricyanide ion is zero at this electrode. Mass transfer limitations do not occur at the anode, if its transfer area is very large relative to that at the cathode. Under these conditions, the mass transfer coefficient is given by

$$K=(i/n_eFAC_b) \tag{7}$$

To overcome ion-migration effects in a potential field, the potassium ferricyanide/ferrocyanide solutions are dissolved in a strong electrolyte, in this case aqueous caustic. When the concentration of this unreactive electrolyte is high enough compared with the concentration of ferricyanide ion, the transfer of ferricyanide ion is by ordinary diffusion or by the ordinary mass transfer mechanism with constant composition at the wall.

To obtain heat transfer coefficients, it is assumed that an analogy exists between heat and mass transfer, the analogous heat transfer system corresponding to that of constant wall temperature. The analogy suggests that the *j*-factors for heat and mass transfer have the same dependence on the fluid mechanical parameters (such as Reynolds number). This means that

$$\left(\frac{h}{C_p\rho u}\right)\cdot(Pr)^m=\frac{K}{u}(Sc)^m \tag{8}$$

and hence

$$h=KC_p\rho(Sc/Pr)^m$$

In turbulent pipe flow, $m=2/3$ but in the system under study the value of this exponent is unknown. Previous experimental studies[2,11] suggested that the exponent of the Prandtl number in a *j*-factor correlation is zero. On the other hand, considering the penetration model, the exponent is 1/2. This coefficient was used here, although obviously the analogy between heat and mass transfer should be better established before the results of this study can be confidently extrapolated to heat transfer systems. The results are presented with this reservation.

3. Experimental Results and Discussion

3. 1 Limiting current experiment

Before meaningful measurements can be made on the systems, the experimental conditions under which the limiting current assumption can be made must be established. This was determineded as follows:

At a typical operating condition (rotational speed, liquid flow rate) a series of measurements was made of current density at particular settings of cathode potential. Since the instantaneous current varies with time (see Fig. 4), it was recorded continuously for each cathode potential. The maximum and minimum currents (labelled $\phi=0°$ and $\phi=90°$, respectively) are plotted as a function of voltage in **Fig. 3**. The limiting current region is that voltage range over which the current is constant.

The results are shown in Fig. 3 and it can be seen that this characteristic constant current occurs when the voltage is maintained between the limits of 1.05 to 1.3 volts. The sharp increase in current at voltages above this is caused by the discharge of a secondary reaction. A voltage of about 1.2 V was used in the experiments of this investigation.

3. 2 Time average heat transfer coefficient

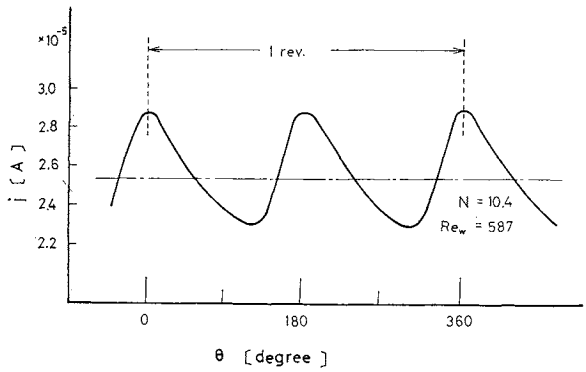

Fig. 4 Typical response from experiment

The instantaneous current as measured at one cathode is plotted, in **Fig. 4**, against angle (transformed time scale) where the angle is the apparent one between the wiper blade and the radius vector through the electrode. In this plot, it is assumed that the maximum mass transfer rate occurs when the wiper blade passes over the electrode. By fixing a microswitch at an appropriate position on the shaft, and with an appropriate electrical current, the actual time when the blade passed the electrode was recorded on the chart simultaneously. It was found that only at the lowest rotational speed did the maximum current coincide nearly with the $\phi=0°$. As the speed of rotation increased, the wiper blade passed the electrode somewhat before the maximum was reached and this time difference increased as the rotational speed increased. This point will be discussed later.

Since the instantaneous current is a direct measure of the instantaneous mass transfer coefficient, it is possible to obtain an integrated average mass transfer coefficient by integrating these point values to give the integrated average current to be used in Eq. (7). The averaged heat transfer coefficient is obtained from Eq. (8).

Figure 5 shows the variation of the integrated average current with axial position as measured by the four different electrodes operating separately. Only at the uppermost electrode is there a slight decrease, and since this decrease is greater at lower rotational speeds it can be attributed to liquid distribution (entrance) effects. The results reported here are for lower electrodes only.

Figure 6 presents the average heat transfer coefficients for all runs against rotation speed. For comparison, the predictions from theory (Eq. (4)) and from Bott and Azoory[2] (Eq. (6)) are also shown. Since the temperature of the fluid was constant, the Prandtl number is constant and according to the Bott and Azoory correlation the results should be represented by the dashed line. Note that our measurements suggest a slightly lower slope of about 0.45 (the slope or the exponent of N should be 1/2

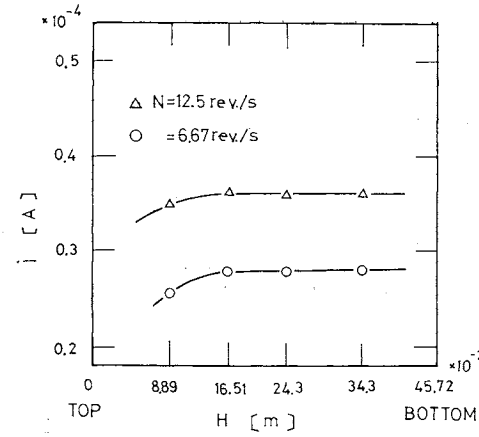

Fig. 5 Axial variation of integrated average current (mass transfer coefficient) from top to bottom of exchanger

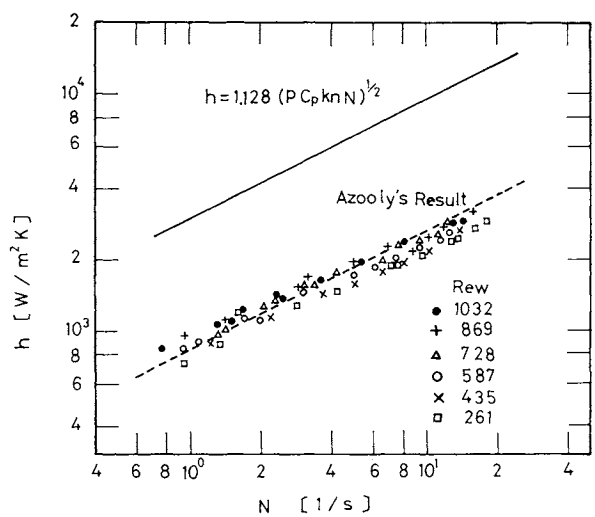

Fig. 6 Variation of heat transfer coefficient with rotational speed

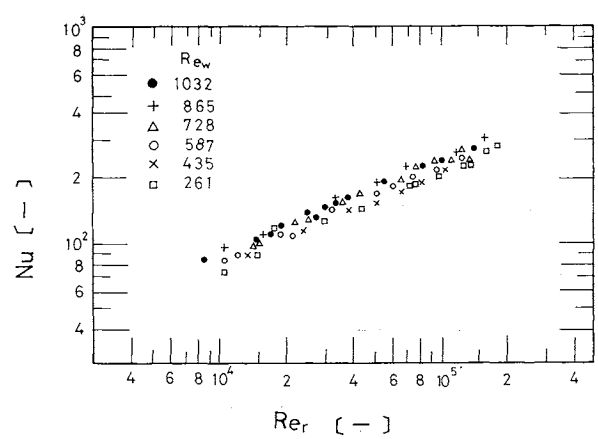

Fig. 7 Variation of Nusselt number with rotational Reynolds number

according to Eqs. (5) and (6)). There is also considerably more scatter of the results than would be expected given the accuracy of the experimental technique. Indeed, there seems to be an apparent effect of mass flow rate, which is more apparent in **Fig. 7**;

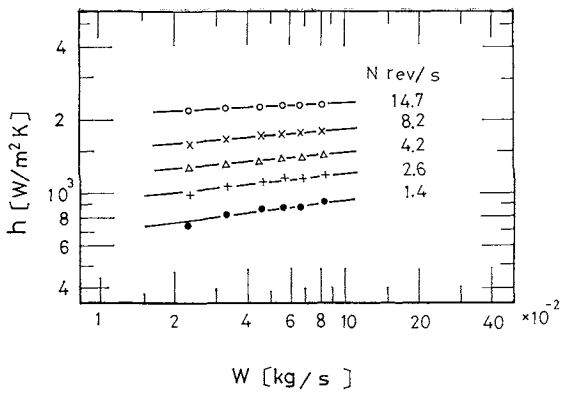

Fig. 8 Variation of heat transfer coefficient with mass flow rate of liquid at various rotational speeds

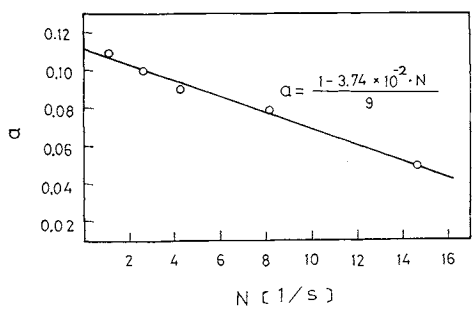

Fig. 9 Correlation of exponent a with rotational speed

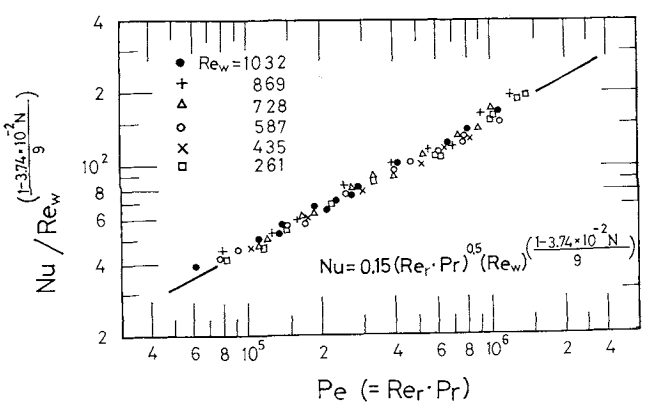

Fig. 10 Plot of data according to correlating Eq. (11)

a plot of Nusselt number vs. rotational Reynolds number.

To investigate this mass flow rate effect, the average heat transfer coefficient was plotted against mass flow rate for constant rotational speed, as shown in **Fig. 8.** It is seen that, contrary to theory, the heat transfer coefficient does show a dependence on mass flow rate and the magnitude of this variation is greatest at the lowest rotational speeds. This dependence on flow rate can be expressed as a power low, viz:

$$h=W^a \tag{9}$$

where a is the slope of the h versus W plot (Fig. 8). When this exponent is plotted against N (**Fig. 9**), it is shown to be a linear function of rotational speed and can be expressed by

$$a=1-3.74\times10^{-2}\cdot N/9 \tag{10}$$

The exponent extrapolates to a value of 1/9 at $N=0$. This is exactly the exponent found by Boys and McAdams[4] in their correlation of heat transfer coefficient versus flow rate of liquid films flowing down the inside of a vertical cylinder (forced convection by gravity only). This suggests that although centrifugal forces obviously dominate the heat transfer/fluid mechanical phenomena, gravity still plays a secondary role and a relatively lesser one as rotational speed increases.

The effect of flow rate may be expressed in dimensionless form through the Reynolds number. A plot of Nu/Re_w^a vs. Péclet number as indicated in **Fig. 10** provides the desired correlation. Note that the results show very little scatter about the best straight line through the data as represented by the equation

$$Nu=0.15(Re_r\cdot Pr)^{0.5}Re_w^a \tag{11}$$

Now the exponent on the Péclet number, as determined from the best line fit, is 1/2, as theory suggests.

3. 3 Instantaneous Heat Transfer Coefficient

With the electrochemical technique, the variation of current with time is a direct indication of the variation of the instantaneous heat transfer coefficient. This variation is shown in **Fig. 11**, where, for a number of selected rotational speeds, the instantaneous current is plotted against a dimensionless time (time normalized with respect to N/n, the time between scrapings at a particular point). Zero time is arbitrarily taken at the time when the current is minimum. The experimental system allowed a measurement of when the blade passed directly over the electrode and this observation is indicated by the arrow on the plot. There are a number of points worth noting:

(i) The time period from the minimum to the maximum current increases with rotational speed.

(ii) The maximum current (instantaneous heat transfer coefficient) does not occur at the time the blade passes over a point, but a finite time after. This lag time increases with rotational speed.

(iii) The minimum heat transfer coefficient occurs at a fixed dimensionless time just before the blade passes the point. This suggests that the minimum heat transfer coefficient occurs as the liquid fillet, which has been observed to exist on the foward face of the blade, passes over the point in question.

Although the time-averaged coefficients have already been shown to be approximately a third of those predicted by the conduction model, it is informative to compare the variation of the calculated instantaneous values with those observed (comparing shape of

curves). This is best done by normalizing the calculated values relative to the calculated minimum and then plotting the variation of this normalized heat transfer coefficient or current against normalized time in Fig. 11*. There is no question that the observed variation is quite different from that predicted by the conduction model. It can therefore be said that the current model has been proven to be inadequate on both counts, i.e.

(i) for predicting the average heat transfer coefficient and (ii) for predicting general shape of variation of the instantaneous coefficient with time.

Conclusions

The conclusions and contributions of this study can be summarized as follows:

(i) The electrochemical technique has been used successfully to study the transport phenomena in a scraped-film heat exchanger.

(ii) The time-averaged heat transfer coefficients for a two-bladed scraped film heat exchanger may be predicted from the equation

$$Nu=0.15(Re_r \cdot Pr)^{0.5} Re_w^a$$

with $a=(1-3.74\times10^{-2}N)/9$. This correlation suggests that both centrifugal and gravitational forces are important, the latter being of lesser importance as rotational speed is increased.

(iii) Since the recommended correlation represents the data obtained by Bott and Azoory for pure heat transfer quite well, and since it was based on an analogy which required the heat and mass transfer coefficients to vary as the square root of the Prandtl and Schmidt numbers, it is suggested that the proposed correlation may have wider applicability than might be suggested by the limited range of physical properties which have been investigated here. More experimental work in this area is obviously required.

(iv) The observed variation of the instantaneous heat transfer coefficient with time is quite different from that predicted by the unsteady conduction model. Therefore, there is a need for developing a model which accounts more realistically for the actual fluid mechanical behavior of the fluid in the exchanger.

Nomenclature

A	= electrode area	[m²]
a	= exponent defined by Eq. (9)	
C_p	= heat capacity	[J/kg·K]
C_b	= bulk concentration of solution	[mol/m³]
d	= inner diameter of exchanger	[m]
F	Faraday's constant	[coulomb/mol]
f	= factor in Eq. (6)	
h	= heat transfer coefficient	[W/m²·K]

* Note that this method of plotting provides the same curve regardless or rotational speed.

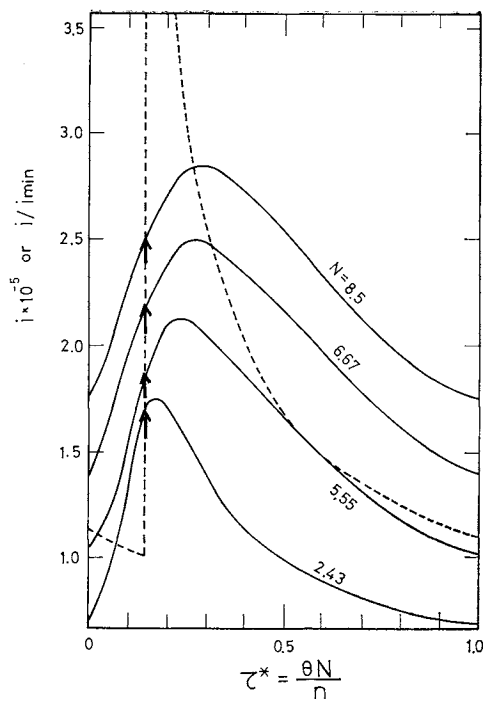

The arrow on each curve is the observed point where the blade is just passing over the electrode. The dashed curve is the plot of the instantaneous current divided by the minimum curve as calculated from the unsteady state conduction model of Kool[8].

Fig. 11 Plot of instantaneous current against dimensionless time for selected rotational speeds

f	= electrical current	[amp.]
K	= mass transfer coefficient	[m/s]
k	= thermal conductivity	[W/m·K]
m	= exponent of the Prandtl and Schmidt number	
N	= rotational speed	[1/s]
Nu	= Nusselt number hd/k	
n	= number of scraped blades on rotating shaft	
Pe	= Péclet number $Re_r \cdot Pr$	
Pr	= Prandtl number $C_p\mu/k$	
Re_w	= flow Reynolds number $4w/\pi d\mu$	
Re_r	= rotational Reynolds number $d^2nN\rho/\mu$	
T, T_w, T_b	= temperature, wall temperature, fluid bulk temperature	[K]
u	= velocity	[m/s]
V	= applied voltage	
W	= mass flow rate	[kg/s]
x	= distance from wall	[m]
θ, θ_c	= time, contact time	[s]
μ	= viscosity	[kg/m·s]
ρ	= fluid density	[kg/m³]
τ^*	= actual time/time between scrapings $\theta N/n$	
ϕ	= angle	

Literature Cited

1) Azoory, S. and T. R. Bott: *Can. J. Chem. Eng.*, **48**, 373 (1970).
2) Bott, T. R., S. Azoory and K. E. Porter: *Trans. Inst. Chem. Eng.*, **46**, T33, T37 (1968).
3) Bott, T. R. and J. J. B. Romero: *Can. J. Chem. Eng.*, **44**,

226 (1966).
4) Boys, G. S. and W. H. McAdams: *Ind. Eng. Chem.*, **29**, 1240 (1937).
5) Harriott, P.: *Chem. Eng. Prog. Symp. Ser.*, **29**, 137 (1959).
6) Higbie, R.: *Trans. AIChE*, **31**, 365 (1935).
7) Kern, D. Q. and H. J. Karakas: *Chem. Eng. Prog. Symp. Ser.*, **29**, 141 (1959).
8) Kool, J.: *Trans. Inst. Chem. Engrs.*, **36**, 259 (1958).
9) Lustenader, E. L. *et al.*: *Trans. ASME J. Heat Transfer*, **81C**, 297 (1959).
10) Mizushina, T.: "Advances in Heat Transfer", Vol. 7, Academic Press (1971).
11) Skelland, A. H. P., D. R. Oliver and S. Tooke: *Brit. Chem. Eng.*, **7**, 346 (1962).

ABSORPTION OF DILUTE NITRIC MONOXIDE IN AQUEOUS SOLUTIONS OF Fe(II)-EDTA AND MIXED SOLUTIONS OF Fe(II)-EDTA AND Na_2SO_3

MASAAKI TERAMOTO, SHIN-ICHIRO HIRAMINE, YUZO SHIMADA, YOSHIHIRO SUGIMOTO AND HIROSHI TERANISHI
Department of Industrial Chemistry, Faculty of Industrial Arts, Kyoto Institute of Technology, Matsugasaki, Kyoto 606

Absorption rates of NO in aqueous solutions of Fe(II)-EDTA chelate as well as in mixed solutions of Fe(II)-EDTA and Na_2SO_3 were measured using a stirred vessel with a free flat gas-liquid interface and a bubble column.

The rate constants of the complexing reaction of NO with Fe(II)-EDTA were determined on the basis of the theory of gas absorption accompanied by a reversible reaction. The chemical equilibrium constants were also determined at various pH values. It was found that the rate constant was of the order of 10^8 l/g-mol·sec and that the equilibrium constant was about 10^6 l/g-mol at 25°C. These values are much higher than the corresponding values of the reaction between NO and Fe(II) in the absence of EDTA.

The mechanism of the absorption of NO in mixed solutions of Fe(II)-EDTA and Na_2SO_3 was deduced from the observation that the absorption efficiency decreased in the early stage of absorption and then increased to some steady value. The absorption rates were satisfactorily explained on the assumption that NO coordinates to Fe(II) (EDTA) (SO_3^{2-}) irreversibly.

It was also found that the absorption rate of NO in the aqueous solution of Fe(II)-EDTA was much higher than those of other liquid absorbents so far investigated.

Introduction

Removal of NO_x in flue gases has recently become important preventing air pollution, and many processes to remove NO_x by liquid absorbents as well as solid-catalyzed reactions have been proposed. Recently it was shown that aqueous solutions of Fe(II) chelates, especially Fe(II)-EDTA chelate, are promising liquid absorbents of NO because of their very fast absorption rates and easy regeneration[4,14].

When NO is absorbed into Fe(II) chelate solutions, it coordinates to Fe(II). As absorption proceeds, the absorption rate decreases because of the consumption of Fe(II)-EDTA and the reversible nature of the complexing reaction. However, if some reducing agents such as Na_2SO_3, which can reduce NO coordinating to Fe(II), are added to the solution, high absorption rate can be maintained.

The purpose of this paper is to investigate the chemical equilibrium and the kinetics of the complexing reaction between NO and Fe(II)-EDTA and the absorption mechanism of NO both in the absence and in the presence of Na_2SO_3, using a bubble column and a stirred vessel with a free flat gas-liquid interface. The effect of experimental conditions on the conversion of NO to N_2O was also examined.

Received September 16, 1977. Correspondence concerning this article should be addressed to M. Teramoto. S. Hiramine is now with Kao Soap Co., Ltd., Tokyo 103 and Y. Shimada is at The Inst. for Chem. Res., Kyoto Univ., Kyoto 611.